

PACS numbers: 42.55.Lt; 42.60.By; 28.41. – i
DOI: 10.1070/QE2009v039n06ABEH014030

Successive composition of two laser channels upon excitation of He – Ar – Xe (2.03 μm) and Ar – Xe (1.73 μm) mixtures by uranium fission fragments

A.A. Pikulev, V.M. Tsvetkov, P.V. Sosnin, A.A. Sinyanskii

***Abstract*. The operation efficiency of the scheme with successive composition of two laser channels upon excitation of the active medium by uranium-235 fission fragments is studied experimentally and numerically. For the He : Ar : Xe = 380 : 380 : 1 mixture (at a pressure of 1 atm and the lasing wavelength $\lambda = 2.03$ μm) the maximum lasing power of a double channel (1 kW) is almost twice that of a single channel (540 W). Calculations show that in the case of ideal composition (without losses on mirrors) the lasing power of the double channel can be increased to 1.2 kW. For the Ar : Xe = 380 : 1 mixture (the pressure is 0.5 atm, $\lambda = 1.73$ μm) the maximum lasing power of the double channel (620 W) is slightly above that of the single channel (520 W), which is caused by the losses on aluminum mirrors employed for channel doubling and by a negative effect of optical inhomogeneities. In the case of ideal composition, the lasing power can be increased to 830 W.**

Keywords: *distributed loss coefficient, active laser medium, nuclear-pumped lasers, multichannel laser system, small-signal gain, saturation intensity, composition of laser channels.*

1. Introduction

The development of powerful laser facilities with an active medium pumped by uranium fission fragments {nuclear-pumped lasers (NPLs) [1]} is connected with a problem of reducing the number of simultaneously generated laser beams to a reasonable limit. This problem arises from the specificity of NPLs: any sufficiently powerful facility should be multichannel.

One way to solve this problem is integration of several laser cells with the active laser medium into a complex cavity. During lasing, a common wave field is produced in the complex cavity, which embraces all the cells and radiation is coupled out in the form of a single laser beam. In paper [2], two methods for combining laser channels were suggested for a cw NPL, which were called parallel and successive composition of laser channels by analogy with parallel and series connection of elements in an electrical circuit (see Fig. 1).

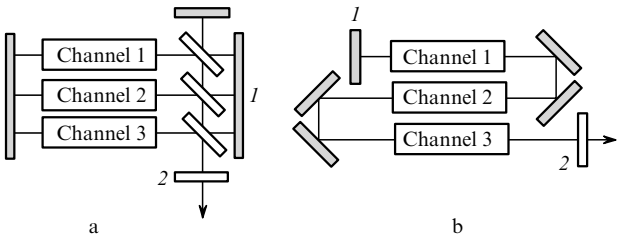

Figure 1. Schemes for parallel (a) and successive (b) composition of three laser channels [2]: (*1*) highly reflecting mirror; (*2*) semitransparent mirrors.

The scheme of parallel composition of laser channels shown in Fig. 1a is a variant of the radiation phasing scheme [3] for the case of strong coupling between the channels with the transversal radiation coupling through a single beam. This scheme was studied theoretically in [4] and first experimental results were presented in review [5].

In a successive composition scheme, the active medium of generator is enlarged by virtue of corner-type reflectors (see Fig. 1b). This scheme is widely used in industrial CO_2 lasers [6]. The successive composition scheme for NPLs was sufficiently well studied analytically [4] and to some extent experimentally [7, 8]. In experiments [7] with successive composition of two laser channels the lasing threshold was about twice lower and the output power was twice greater than for a single channel. The result of the successive composition of three laser channels was not so good: the power of the combined generator proved lower than that of a single laser channel [8]. There may be several reasons for such a low composition efficiency. We will mention only the accumulation of even-order optical inhomogeneities, which occurs at an increased number of laser channels and incomplete compensation for odd-order inhomogeneities (in particular, from an optical wedge) upon composition of an odd number of channels.

Thus, the scheme of successive composition for NPLs has not been experimentally studied yet. The main drawbacks in the experiments [7, 8] are nonoptimal laser cavities of single and double channels, which hinder the determination of the composition scheme efficiency. On the other hand, optimisation of a successive composition scheme requires changing the cavity mirrors in each experiment, which is difficult in the laser setups of the LM type [9]

A.A. Pikulev, V.M. Tsvetkov, P.V. Sosnin, A.A. Sinyanskii Russian Federal Nuclear Center 'All-Russian Research Institute of Experimental Physics', prosp. Mira 37, 607190 Sarov, Nizhnii Novgorod region, Russia; e-mail: pikulev@expd.vniief.ru

Received 22 December 2008
Kvantovaya Elektronika **39** (6) 494 – 500 (2009)
Translated by N.A. Raspopov

because of the radiation safety limitations and complicated adjustment of laser cavities and the whole optical tract. Thus, the two-channel LUNA-2M laser facility [10] residing in the ground hall of the VIR-2M pulse reactor [11] was used to perform a series of experiments on optimising the successive composition scheme for two laser channels.

This paper is devoted to experimental and analytical study of energy parameters of the successive composition scheme for two laser channels. He–Ar–Xe and Ar–Xe laser mixtures were used in the experiments. The parameters of these active media (the small-signal gain, saturation intensity, and distributed loss coefficient) were studied versus the pump power. The efficiency of the two channel composition scheme was calculated and optical inhomogeneities and lasing power for single and double laser channels were simulated. The results obtained were compared with the experimental data.

2. Experimental

Experiments were carried out on the LUNA-2M two-channel nuclear-pumped laser facility [10]. Two plane aluminum plates of size 6×200 cm were placed inside each cavity at a distance of 2 cm from each other. The internal plate surfaces were deposited with the ^{235}U oxide-protoxide layers with the surface density of ~ 3 mg cm^{-2}. The VIR-2M water pulsed reactor [11] was used as a source of neutrons. The half-height pulse duration was 3.2 ms at the reactor energy release of 54 ± 2 MJ. The average neutron flux density at the maximum of the reactor pulse recalculated to thermal neutrons was 2×10^{15} cm^{-2} s^{-1}, which for both mixtures employed in the experiments corresponds to a mean specific pump power of ~ 40 W cm^{-3}.

In each channel of the LUNA-2m facility [10], one adjusting bellows coupling unit was replaced by a unit with a Brewster window, which provided a linear polarisation of laser radiation with the polarisation vector directed vertically. The transmission of the Brewster windows was 93 % at normal beam incidence for the wavelengths 2.03 and 1.73 μm.

The highly reflecting dielectric mirrors had a radius of 10 m and reflection coefficients of above 99.7 % at the operation wavelength. The coupling mirrors of the optical cavity were plane dielectric mirrors with various reflection coefficients.

The scheme of experiments with two successively combined laser channels is shown in Fig. 2. Two aluminum mirrors with the reflection coefficients of 96 % – 97 % were used for optical composition of the channels. Two laser mixtures were used: the He:Ar:Xe = 380:380:1 mixture at the total pressure of 1 atm and the lasing wavelength $\lambda =$ 2.03 μm (the $5d[3/2]_1^o \rightarrow 6p[3/2]_1$ transition in the xenon atom) and the Ar:Xe = 380:1 mixture at the pressure of 0.5 atm, $\lambda = 1.73$ μm (the $5d[3/2]_1^o \rightarrow 6p[5/2]_2$ transition).

Three series of experiments were carried out in which we investigated the far- and near-field radiation distribution for a single laser channel, studied the evolution of the laser beam cross-section area during the reactor pulse action, and optimised the lasing power for the single and double channels by varying the reflection coefficient of the outcoupling mirror.

The near- and far-field radiation distributions were investigated by means of the Ragulsky wedge. In the experiments, four autographs of the laser beam were obtained on a carbon paper with the successive image expositions 1 : 0.5 : 0.25 : 0.13 at $\lambda = 2.03$ μm and 1 : 0.6 : 0.3 : 0.1 at $\lambda = 1.73$ μm.

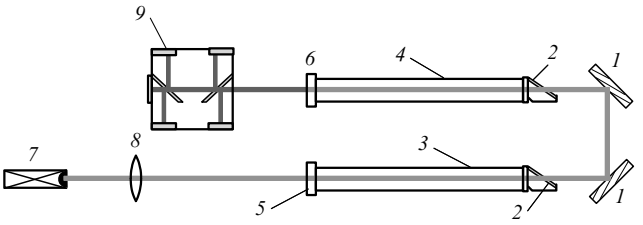

Figure 2. Optical scheme for measuring radiation parameters of the double laser channel: (*1*) slewing aluminum mirrors; (*2*) Brewster windows; (*3*) first channel; (*4*) second channel; (*5*) semitransparent outcoupling mirror; (*6*) highly reflecting spherical mirror; (*7*) energy meter; (*8*) focusing lens; (*9*) photodetector unit.

The experiments show that at $\lambda = 2.03$ μm almost all the far-field radiation energy (more that 90 %) is concentrated in the angle ranges $|\phi_x| < 6$ mrad and $|\phi_y| < 5$ mrad and at $\lambda = 1.73$ μm in the ranges $|\phi_x| < 5$ mrad and $|\phi_y| < 4$ mrad.

At $\lambda = 2.03$ μm the near-field radiation fills the rectangular region $|x| < 20$ mm and $|y| < 8$ mm almost uniformly; the laser beam cross-section area is ~ 6.4 cm^2. At $\lambda =$ 1.73 μm about 90 % of the energy is concentrated in the range $|x| < 17$ mm and $|y| < 7$ mm; the cross-section area is ~ 4.8 cm^2.

Evolution of the near-field laser beam cross section was studied by the method of a moving target. Horizontal and vertical scans of laser beam autographs were obtained in the scale 1 : 4. Analysis of the autographs shows that the lasing pulse can be divided into three phases: lasing onset, evolution, and a developed lasing stage.

At the first stage, lasing starts in the near-axis region of the laser channel at low-order modes. In the evolution phase, a sufficiently fast expansion of the generation region occurs, which occupies almost the entire laser channel at the end of the phase. In the developed lasing phase, the radiation occupies all the active volume and the increase in the lasing power is related to a rising energy per generating mode rather than with a greater number of modes.

To optimise the lasing parameters at $\lambda = 2.03$ μm in studying a single channel we carried out ten experiments with outcoupling mirrors having various reflection coefficients. In studying the double channel scheme we performed six such experiments. In studying the single and double laser channel schemes at $\lambda = 1.73$ μm, we carried out four experiments in each case.

Figs 3 and 4 show the dependences of the laser energy and maximum power on the reflection coefficient of the outcoupling mirror. The maximum energy parameters of lasing are given in Table 1. One can see from Figs 3 and 4 that in passing from the single to double laser channel the optimal reflection coefficient of the outcoupling mirror falls from ~ 70 % to 40 % – 50 %. At $\lambda = 2.03$ μm, a noticeable reduction in the laser energy and power is only observed if the reflection coefficient is as low as 10%. At $\lambda = 1.73$ μm, the reduction in the energy parameters of the two-channel scheme occurs at the reflection coefficient lower than 30 %.

Table 1. Maximum lasing energy parameters.

λ/μm	Mixture	Pressure/atm	Channel	r_{opt} (%)	E_{max}/J	P_{max}/kW
2.03	He : Ar : Xe = 380 : 380 : 1	1	single	71.4	1.46	0.54
			double	45.5	1.81	1.0
1.73	Ar : Xe = 380 : 1	0.5	single	67.7	0.96	0.52
			double	46.8	1.08	0.62

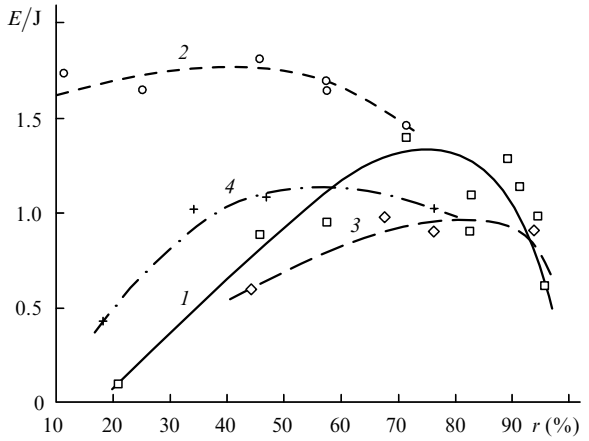

Figure 3. Generation energy E versus the reflection coefficient of outcoupling mirror for a single channel (*1*, *3*) and double channel (*2*, *4*) at $\lambda = 2.03$ μm (*1*, *2*) and 1.73 μm (*3*, *4*). Dots are the experimental results and curves are approximations.

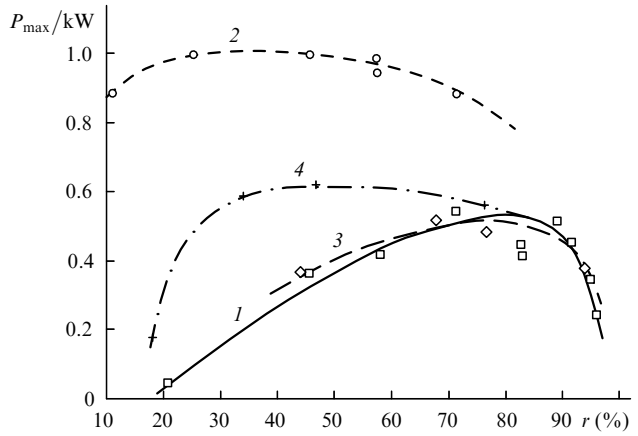

Figure 4. Maximum lasing power P_{max} versus the reflection coefficient of outcoupling mirror for a single channel (*1*, *3*) and double channel (2, 4) at $\lambda = 2.03$ μm (*1*, *2*) and 1.73 μm (3, 4). Dots are the experimental results and curves are approximations.

3. Calculation

3.1 Basic relations

A thorough theoretical study of successive composition of several laser channels is given in [4]. Thus, below we only present the basic relations used in our calculations.

Lumped losses in the cavity comprising N successive identical laser channels include active and adverse losses determined by the coefficients

$$k_0 = \frac{1}{2NL}\ln\frac{1}{r_1 r_2}, \quad k_N = \frac{N-1}{NL}\ln\frac{1}{T}, \tag{1}$$

where $r_{1,2}$ are the reflection coefficients of cavity mirrors; L is the length of a single laser cell; and T is the transmission of the optical element used for composition of channels.

At $T \approx 1$ the lasing power of the complex generator can be found from the approximate formula similar to the Rigrod formula [12]:

$$P_N^{out} \approx k_0 V_N I_s \left(\frac{\alpha_0}{k_0 + \rho_{eff}}\right), \quad \rho_{eff} = \rho + k_N, \tag{2}$$

where V_N is the active volume of the laser (the volume of the laser channels involved in radiation); α_0 is the small-signal gain; I_s is the saturation intensity; and ρ (ρ_{eff}) is the distributed loss coefficient (effective coefficient).

The optimal cavity parameters and the corresponding optimal (maximum) lasing power N of the combined channels can be found from the expressions [4]

$$(r_1 r_2)_{opt} = \exp\left[-2NL\rho_{eff}^{1/2}\left(\alpha_0^{1/2} - \rho_{eff}^{1/2}\right)\right],$$
$$P_{opt}^{out}(N) = V_N I_s \left(\alpha_0^{1/2} - \rho_{eff}^{1/2}\right)^2. \tag{3}$$

The efficiency of combinations of several laser channels was characterised by the parameter introduced in [4]

$$\eta_N = \frac{P_{opt}^{out}(N)}{N P_{opt}^{out}(1)}. \tag{4}$$

By using Eqn (3), we reduce (4) to the form

$$\eta_N = \frac{V_N}{N V_1}\left(\frac{\alpha_0^{1/2} - \rho_{eff}^{1/2}}{\alpha_0^{1/2} - \rho^{1/2}}\right)^2, \tag{5}$$

where V_1 is the active volume of the optimised single laser channel.

3.2 Parameters of laser active media

The parameters of laser active media were found experimentally by the calibrated loss method [12]. In least squares calculations, modified Rigrod formula (2) was used from which the parameters α_0, ρ, ρ_{eff} and saturation power $P_s = \langle S_N \rangle I_s$ were determined, where $\langle S_N \rangle = V_N/(NL)$ is the average cross-section area of the laser beam inside the cavity.

Analysis of the experimental results for the He : Ar : Xe = 380 : 380 : 1 mixture (at the pressure of 1 atm and $\lambda = 2.03$ μm) shows that $\alpha_0 \propto q$ (where q is the specific pump power) and at the maximum of pump pulse we have $\alpha_0 \sim 1.1$ m^{-1}, which is close to the values obtained earlier [13]. For a single channel the average distributed loss coefficient in the range of specific pump powers 0–40 W cm^{-3} is ~ 0.01 m^{-1}.

In the case of the double channel the average effective distributed loss coefficient is 0.025 m^{-1}. For $\rho \approx 0.01$ m^{-1} the lumped adverse loss coefficient is $k_2 \approx 0.015$ m^{-1}, which corresponds to the reflection coefficient of $\sim 97\,\%$ for

aluminum mirrors. This value coincides with the tabulated data in [14].

The time dependence of the saturation power for a single channel well correlates with the area of a near-field laser beam autograph. At the lasing pulse maximum the saturation power is 310 W and the saturation intensity is approximately 50 W cm^{-2}.

For the double channel the behaviour of the saturation power significantly differs from the single-channel case. At the leading edge of a pump pulse after the lasing onset the saturation power rapidly rises to ~ 50 W, then slowly increases to ~ 100 W which is followed by a sharp jump to 320 W. At the trailing edge of the pump pulse the saturation power for the double channel is lower compared to the single channel. This behaviour of power P_s is related, first of all, to variations in the average cross section of the laser beam $\langle S_N \rangle$ during the generation of the pulse, which is determined by optical inhomogeneities in the laser channel.

For the Ar:Xe = 380:1 mixture (at the pressure of 0.5 atm and $\lambda = 1.73$ μm) we have $\alpha_0 \propto q^{1/2}$, and at the maximum of the pump pulse $\alpha_0 \approx 0.35$ m^{-1}, which agrees with the results from [13]. The average distributed loss coefficient for the single channel is ~ 0.01 m^{-1} similarly to the case of $\lambda = 2.03$ μm.

For the double channel the effective distributed loss coefficient is 0.04 m^{-1}, which is noticeably greater than in the case of $\lambda = 2.03$ μm. This fact can be explained by a sufficiently low reflectance of aluminum mirrors (~ 94 %) or greater diffraction losses at higher generation modes in the double channel.

The time dependence of the saturation power for both single and double channels is of spiking character at the leading edge of the pump pulse and the maximum saturation power is shifted to the pulse onset. This may result from optical inhomogeneities or active medium heating. The maximal saturation power for the single channel is ~ 1160 W and for the double channel it is 1180 W. The saturation power at the maximum of the lasing pulse is approximately 240 W cm^{-2}.

3.3 Efficiency of the composition scheme with two channels

Generation pulses with the maximum power are presented in Fig. 5 ($\lambda = 2.03$ μm) and Fig. 6 ($\lambda = 1.73$ μm) for the single and double channels. The calculated lasing power is also shown for an optimised double channel in the case of ideal composition (the reflection coefficient of the optical elements is assumed 100 %). In the calculations we used the experimentally found parameters α_0, ρ, ρ_{eff}, and P_s for the active media.

One can see from Fig. 5 that at $\lambda = 2.03$ μm the maximal lasing power for the double channel (1 kW) is approximately twice that for the single channel (540 W). Calculations show that in the case of ideal composition the lasing power of the double channel can be increased to 1170 W.

At $\lambda = 1.73$ μm (see Fig. 6) the maxima of lasing pulses in the single and double channels are observed at the leading edge of the pump pulse. This can be explained by heating of the Ar–Xe active medium and influence of the distributed negative lens whose plane is parallel to the uranium layers. One can see from Fig. 6 that at $\lambda = 1.73$ μm at the instant $t \sim 5.5$ ms an abrupt rise in the double-channel lasing power occurs, whose maximum value (620 W) exceeds, though moderately, the single-channel power (520 W). In the case of ideal composition the maximum lasing power will be 830 W.

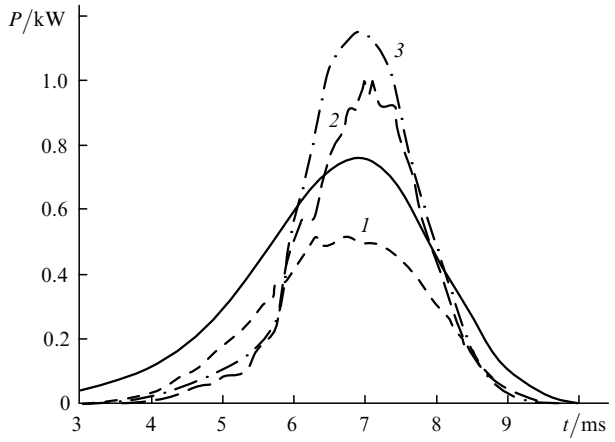

Figure 5. Pulses with the maximum lasing energy for a single (*1*) and double (*2*) channels ($\lambda = 2.03$ μm) and calculated power of the optimised generator at the reflection coefficient of slewing mirrors 100 % (*3*). Solid curve is the shape of reactor pulse.

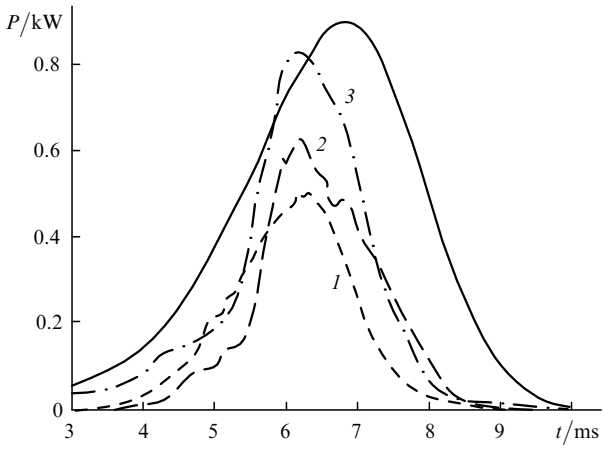

Figure 6. Pulses with the maximum lasing energy for a single (*1*) and double (*2*) channels ($\lambda = 1.73$ μm) and calculated power of the optimised generator at the reflection coefficient of slewing mirrors 100 % (*3*). Solid curve is the shape of reactor pulse.

Figures 7 and 8 present the experimental and calculated efficiencies of channel composition under experimental and ideal (without losses on the optical elements of the composition scheme) conditions. The composition efficiency was determined by expression (4). One can see that the calculation well agrees with the experimental results. It follows from Fig. 7 ($\lambda = 2.03$ μm) that the maximum efficiency (92 %) is obtained at the maximum of the pump pulse. At the trailing edge of the pump pulse the efficiency gradually falls which is related to developing optical inhomogeneities. Estimates show that employment of ideally reflecting mirrors may raise the efficiency to ~ 110 %.

Time evolution of the composition efficiency at $\lambda = 1.73$ μm (see Fig. 8) is of complicated character: curves (*1*) and (*2*) exhibit four steps (at $t = 2.8 - 3.7$ ms, 6–6.5 ms, 8–8.5 ms, and 9.2–9.4 ms) and a sufficiently deep gap (~ 5 ms). The efficiency at the maximum of lasing pulse is ~ 60 %. The calculation results show that under the ideal conditions the efficiency may rise to 83 %.

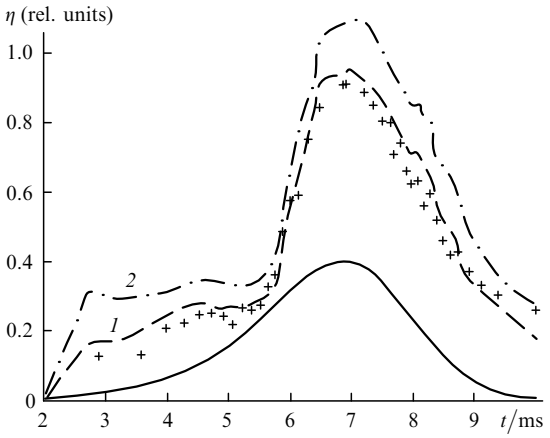

Figure 7. Experimental (dots), calculated (*1*), and limiting calculated (*2*) efficiencies for successive composition of two channels versus time ($\lambda = 2.03$ μm). Solid curve is the shape of reactor pulse.

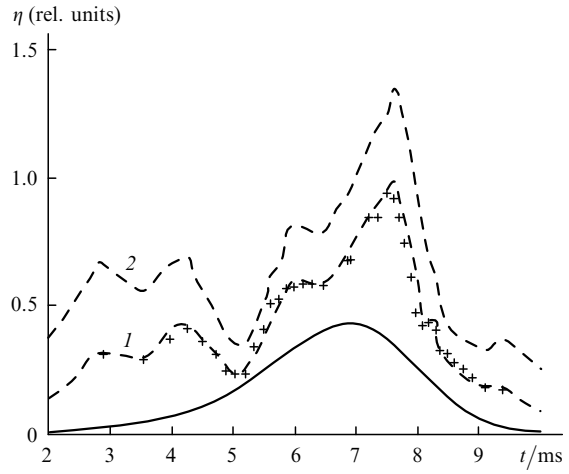

Figure 8. Experimental (dots), calculated (*1*), and limiting calculated (*2*) efficiencies for successive composition of two channels versus time ($\lambda = 1.73$ μm). Solid curve is the shape of reactor pulse.

3.4 Influence of optical inhomogeneities

To estimate the influence of optical inhomogeneities we simulated the time evolution of lasing power for the double channel. The calculations were specific in that we tried to find the active volume V_N numerically rather than from experimental results as was done above.

In this paper the value and distribution of the energy deposition in laser cavities were determined by the method described in [15]. The energy deposition was calculated for the quadratic deceleration law for fission fragments in the approximation of average uranium fission fragment. Under these assumptions the error in determining the energy deposition does not exceed 10 % [16].

Optical inhomogeneities in the laser channels were determined in the small-energy deposition approximation [17] by neglecting the heat conduction. In the central part of the laser channel the refractive index was approximated by a second-order polynomial (for $|x| \leqslant 15$ mm, $|y| \leqslant 5$ mm the error of this approximation does not exceed 3 %) so that we might use matrix optics for describing propagation of radiation [18].

If an optical cavity was stable, i.e., $|J| < 1$, where $J \equiv AD + BC$ ($ABCD$ is the matrix of cavity round trip from left to right [18]) then the lasing power was determined by expression (2) and the volume V_N was assumed equal to the volume of laser active medium occupied by the maximum-order generation mode whose transverse dimension is limited only by the apertures of the laser channel and optical elements.

For unstable cavities ($|J| > 1$) the lasing power was determined by expression (2), where V_N is equal to the maximum volume of laser active medium occupied by the converging and diverging electromagnetic waves and the factor k_N makes allowance, in addition to the losses on optical elements of the composition scheme, for the losses connected with cavity instability:

$$k_N = \frac{1}{NL} \ln \left(\frac{m_x m_y}{T^{N-1}} \right), \tag{6}$$

where m_x and m_y are the optical cavity magnification factors along the x and y axes, respectively [18].

Some calculation results are presented in Figs 9 and 10. Data for the He–Ar–Xe mixture ($\lambda = 2.03$ μm) given in Fig. 9 show that the single channel has one instability region (6.1–6.3 ms) whereas the double channel has three such regions (4–4.5 ms, 6–6.4 ms, and 7.6–7.7 ms). The second and third dips in the time dependence of the lasing power for the double channel are explained by an influence of optical inhomogeneities. The lasing power for the double laser channel was calculated for the outcoupling mirror with the reflectivity 71.7 %.

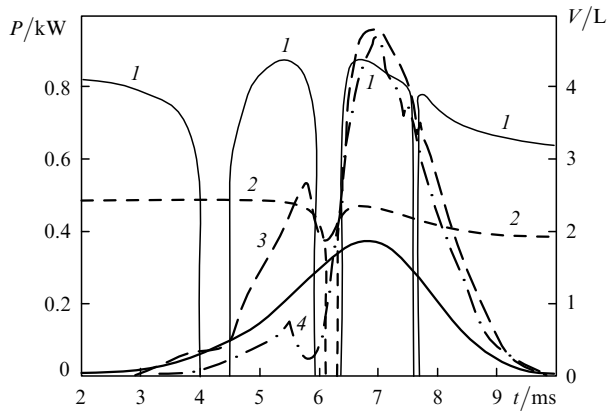

Figure 9. Time dependence of the volume V of the stable region of laser active medium for double (*1*) and single (*2*) channels; calculated (*3*) and experimental (*4*) lasing power ($\lambda = 2.03$ μm). Solid line is the shape of reactor pulse.

The calculations performed for the He:Ar:Xe = 380:380:1 mixture (at the pressure of 1 atm, $\lambda = 2.03$ μm) show that the optical cavity used in the experiments remains stable during the entire reactor pulse when a negative lens arises (x axis). It also remains stable at the maximum of the pump pulse when a positive lens (y axis) arises. This allows us to obtain high energy parameters in the experiment with the double channel at the reactor pulse maximum.

In the case of the Ar–Xe mixture ($\lambda = 1.73$ μm) the single channel has one instability region (5.7–5.9 ms) and the double channel has two such regions (3.7–4.2 ms and 5.5–6 ms) (see Fig. 10). The lasing power was calculated for

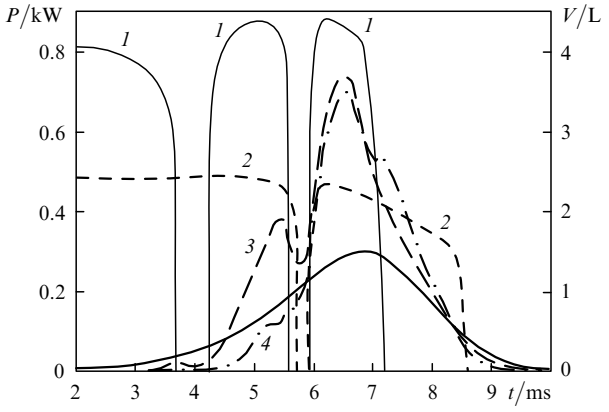

Figure 10. Time dependence of the volume V of the stable region of laser active medium for double (*1*) and single (*2*) channels; calculated (*3*) and experimental (*4*) lasing power ($\lambda = 1.73$ μm). Solid line is the shape of reactor pulse.

the outcoupling mirror with the reflectivity 46.8 %. The cavity of the single channel becomes unstable with respect to a negative lens (x axis) at $t > 8.5$ ms, whereas the double-channel cavity does so at $t > 7.5$ ms. There is a third region of instability for the double channel along y axis (7.2–7.4 ms). However, it is completely masked by the negative-lens instability.

In the Ar:Xe = 380:1 mixture (at the pressure of 0.5 atm, $\lambda = 1.73$ μm), unstable regions arise due to a distributed focusing lens along both the vertical y and horizontal x axes. One can see from Fig. 10 that the optical cavity in this case is not optimal at the instant of lasing pulse maximum which results in a moderate efficiency of composition obtained in the experiments (~ 60%). On the other hand, the low lasing efficiency of the double channel is caused by high losses on aluminum mirrors. Calculations show that by replacing aluminum mirrors by ideally reflecting mirrors the composition efficiency can be increased to 83 %.

One can see from Figs 9 and 10 that for both wavelengths at the leading edge of the reactor pulse the experimental lasing power in the double channel is lower than the calculated value. This may be explained by the fact that the generation initially arises at lower modes in the channel region near the axis. At $t > 6$ ms the experimental and calculated lasing pulses coincide because the generation occupies all the active volume of the laser.

4. Conclusions

The following results have been obtained from the experimental and analytical study of energy parameters of the successive composition scheme for two laser channels on the LUNA-2M nuclear-pumped laser facility:

(i) For the He:Ar:Xe = 380:380:1 active medium (at the pressure of 1 atm), the small-signal gain at $\lambda = 2.03$ μm grows linearly with the specific pump power q and is equal to 1.1 m^{-1} at $q = 40$ W cm^{-3}. The saturation intensity is 50 W cm^{-2} and distributed loss coefficient is ~ 0.01 m^{-1};

(ii) For the Ar:Xe = 380:1 active medium (at the pressure of 0.5 atm), the small-signal gain at $\lambda = 1.73$ μm grows as a square root from the specific pump power and is equal to 0.35 m^{-1} at $q = 40$ W cm^{-3}. The saturation intensity is 240 W cm^{-2} and distributed loss coefficient is ~ 0.01 m^{-1} for the single and ~ 0.02 m^{-1} for the double channels;

(iii) At $\lambda = 2.03$ μm the maximum lasing power and energy for the single channel are 540 W and 1.46 J, respectively. For the double channel, they are 1 kW and 1.81 J, respectively. The composition efficiency obtained with respect to power (at the maximum of lasing pulse) is 92 %. Calculations show that with ideally reflecting mirrors used as optical elements in the composition scheme the power and efficiency of the double channel may increase to 1.2 kW and 110 %, respectively;

(iv) At $\lambda = 1.73$ μm the maximum lasing power and energy for a single channel are 520 W and 0.96 J, respectively. For the double channel, they are 620 W and 1.08 J, respectively. The composition efficiency obtained with respect to power (at the maximum of the lasing pulse) is 60 %. In the case of ideal addition scheme the power and efficiency of the double channel may increase to 830 W and 83 %, respectively;

The calculations performed show that the lasing parameters for the double laser channel are substantially affected not only by the losses on optical elements of the addition scheme, but also by optical inhomogeneities arising in the laser channels during the pump pulse. This effect is more pronounced in the active medium of the Ar–Xe laser. In particular, the configuration of the optical cavity used in the experiments was not optimal at the instant of lasing pulse maximum, which resulted in low energy parameters at $\lambda = 1.73$ μm for the double laser channel.

Acknowledgements. The authors thank S.P. Mel'nikov for useful remarks and members of the VIR-2M reactor maintenance group S.F. Mel'nikov, L.Yu. Glukhov, and A.A. Kubasov for the help in carrying out this work.

References

1. Sinyanskii A.A., Melnikov S.P. *Proc. SPIE Int. Soc. Opt. Eng.*, **3686**, 43 (1999).
2. Sinyanskii A.A. *Trudy III Mezhdunarodnoi konferentsii 'Problemy lazerov s yadernoi nakachkoi i impul'snye reaktory'* (Proceedings of the III International Conference on Nuclear-pumped Lasers and Pulsed Reactors) (Snezhinsk, 2003) p. 377.
3. Glova A.F. *Kvantovaya Elektron.*, **33**, 283 (2003) [*Quantum Electron.*, **33**, 283 (2003)].
4. Pikulev A.A., Abramov A.A. *Proc. SPIE Int. Soc. Opt. Eng.*, **6263**, 186 (2006).
5. Pikulev A.A., Patyanin S.V., Sinyanskii A.A., Sosnin P.V., Turutin S.L., Tsvetkov V.M. *Proc. SPIE Int. Soc. Opt. Eng.*, **6938**, 69380D (2008).
6. Abilsiitov G.A., Velikhov E.P., Golubev V.S., et al. *Moshchnye gazorazryadnye CO_2-lazery i ikh primenenie v tekhnologii* (High-Power Gas-Discharge CO_2-Lasers and their Applications in Technology) (Moscow: Nauka, 1984).
7. Patyanin S.V., Lisenkov A.V., Pikulev A.A., Sinyanskii A.A., Grigor'ev V.D., Limar' Y.M., Sosnin P.V., Turutin S.L., Tsvetkov V.M. *J. Opt. Technol.*, **69**, 472 (2002).
8. Patyanin S.V., Pikulev A.A., Sinyanskii A.A., Turutin S.L., Tsvetkov V.M. *Sbornik dokladov II nauchnoi konferentsii 'Molodyozh v nauke'* (Reports of the II Scientific Conference 'Youth in Science') (Sarov, 2003) p. 345.
9. Patyanin S.V., Lisenkov A.V., Pikulev A.A., Sinyanskii A.A., Grigor'ev V.D., Limar' Yu.M., Sosnin P.V., Turutin S.L., Tsvetkov V.M. *Opt. Zh.*, **69** (7), 33 (2002).
10. Voinov A.M., Dovbysh L.E., Krovonosov V.N., Mel'nikov S.P., Mel'nikov S.F., Sinyanskii A.A. *Vopr. Atom. Nauk. Tekh., Ser. Fiz. Yader. Reactor.*, (2/3), 63 (2000).

11. Kolesov V.F. *Aperiodicheskie impul'snye reaktory* (Aperiodic Pulsed Reactors) (Sarov: VNIIEF, 1999).
12. Rigrod W.W. *IEEE J. Quantum Electron.*, **14** (5), 377 (1978).
13. Abramov A.A., Melnikov S.P., Mukhamatullin A.Kh., Pikulev A.A., Sinyanskii A.A., Tsvetkov V.M. *Proc. SPIE Int. Soc. Opt. Eng.*, **5483**, 1 (2004).
14. Jamison J.E., MacFee R.H., Plass J.N., Grubbe R.G., Richards R.J. *Fizika i tekhnika infrakrasnogo izlucheniya* (Physics and Technique of Infrared Radiation) (Moscow: Sov. Radio, 1965).
15. Mat'ev V.Yu. *Zh. Tekh. Fiz.*, **71** (1), 72 (2001).
16. Pikulev A.A. *Zh. Tekh. Fiz.*, **76** (6), 38 (2006).
17. Mat'ev V.Yu., Borovkov V.V., Mel'nikov S.P. *Zh. Tekh. Fiz.*, **71** (1), 79 (2001).
18. Anan'yev Yu.A. *Opticheskie rezonatory i lazernye puchki* (Optical Cavities and Laser Beams) (Moscow: Nauka, 1990).